Volume Title
ASP Conference Series, Vol. **Volume Number**
Author

Multi-Wavelength Implications of the Companion Star in η Carinae

Thomas I. Madura[1], Theodore R. Gull[2], Jose H. Groh[1], Stanley P. Owocki[3], Atsuo Okazaki[4], D. John Hillier[5], and Christopher Russell[3]

[1] *Max-Planck-Institut für Radioastronomie, Auf dem Hügel 69, D-53121 Bonn, Germany*
[2] *Astrophysics Science Division, Code 667, NASA Goddard Space Flight Center, Greenbelt, MD 20771, USA*
[3] *Department of Physics and Astronomy, University of Delaware, Newark, DE 19716, USA*
[4] *Faculty of Engineering, Hokkai-Gakuen University, Toyohira-ku, Sapporo 062-8605, Japan*
[5] *Department of Astronomy, 3941 O'Hara Street, University of Pittsburg, Pittsburg, PA 15260, USA*

Abstract. η Carinae is considered to be a massive colliding wind binary system with a highly eccentric ($e \sim 0.9$), 5.54-yr orbit. However, the companion star continues to evade direct detection as the primary dwarfs its emission at most wavelengths. Using three-dimensional (3-D) SPH simulations of η Car's colliding winds and radiative transfer codes, we are able to compute synthetic observables across multiple wavebands for comparison to the observations. The models show that the presence of a companion star has a profound influence on the observed HST/STIS UV spectrum and H-alpha line profiles, as well as the ground-based photometric monitoring. Here, we focus on the Bore Hole effect, wherein the fast wind from the hot secondary star carves a cavity in the dense primary wind, allowing increased escape of radiation from the hotter/deeper layers of the primary's extended wind photosphere. The results have important implications for interpretations of η Car's observables at multiple wavelengths.

1. Introduction

The 5.54-year periodicity observed in numerous spectral lines, as well as the IR, Visual, and X-ray fluxes, strongly suggests η Carinae is a binary system (Whitelock et al. 2004; Damineli et al. 2008a,b; Fernández-Lajús et al. 2010; Corcoran 2011). Recently, Okazaki et al. (2008, hereafter O08) modeled η Car's *RXTE* X-ray light curve using a three-dimensional (3-D) Smoothed Particle Hydrodynamics (SPH) simulation of the binary wind-wind collision. A key point of O08 is that the fast wind of the secondary star, η_B, carves a cavity in the dense wind of the primary, η_A, allowing X-rays that would otherwise be absorbed to escape into our line-of-sight. This immediately suggests that if the primary wind is sufficiently optically thick in the UV, Optical, or IR waveband, the low-density secondary wind may likewise carve or "bore" a cavity or "hole" in the associated wind photosphere, allowing increased escape of radiation from the hotter/deeper layers.

2. The Bore-Hole Effect

Any bore-hole effect should depend on (1) how close the wind cavity carved by η_B gets to η_A and (2) the apparent size of η_A's photosphere. For a bore-hole effect to occur, the optically thick primary wind photosphere must extend *at least* as far as the separation distance between the primary and the apex of the wind-wind interaction region (WWIR), i.e. if at some point (2) > (1), there is a bore hole.

The separation between η_A and the apex of the WWIR is determined by the dynamics of the colliding winds and the orbit. The absolute minimum distance that η_A's photosphere must extend is the separation between η_A and WWIR apex at periastron:

$$R_{\rm min} \equiv \frac{a(1-e)}{1+1/\sqrt{\eta}}\,, \tag{1}$$

where e is the eccentricity (0.9), a is the orbital semi-major axis length (15.4 AU), and η is the momentum ratio of η_A's wind to η_B's wind. For the parameters of O08, $\eta \approx 4.2$ and $R_{\rm min} \approx 1$ AU. Using the primary mass-loss rate $\dot{M} = 10^{-3}\,M_\odot$ yr^{-1} suggested by Hillier et al. (2001, 2006, hereafter H01 and H06), $\eta \approx 16.67$ and $R_{\rm min} \approx 1.24$ AU.

The apparent size of η_A's wind photosphere is determined by radiative transfer effects. While there are many ways to define this apparent size, a simple way is to use the radial photospheric radius $R_{\rm phot}$ at which the radial optical depth $\tau = 1$:

$$R_{\rm phot} = \frac{\kappa \dot{M}}{4\pi v}\,, \tag{2}$$

where κ is the opacity (units of cm^2 g^{-1}, assumed constant for simplicity), $\dot{M}$ is the mass-loss rate of η_A, and v is the terminal speed of η_A's wind. Assuming $\kappa = 1$ cm^2 g^{-1} and mass-loss rates of $\dot{M} = 2.5\times10^{-4}\,M_\odot$ yr^{-1} and $\dot{M} = 10^{-3}\,M_\odot$ yr^{-1}, $R_{\rm phot} \approx 1.67$ AU and 6.71 AU, respectively. Thus, even for low values of κ of order unity, a bore-hole effect should occur in the η Car system (at least at periastron).

In reality, any bore-hole effect in η Car will be wavelength dependent and occur over a relatively short period of time around periastron. The wavelength dependence is due to the opacity, which determines the size of η_A's photosphere. Figure 1 illustrates this, showing an overlaid plot of the normalized intensity as a function of impact parameter from the center of η_A in each of the wavebands *B, V, R, I, J, H, K, L*.

Since the separation between η_A and the apex of the WWIR varies with orbital phase ϕ, the bore-hole effect is also orbital-phase dependent. At apastron, the separation is $\sim$ 23.6 AU, much larger than η_A in either the K- or B-band. Because of the large orbital eccentricity, this separation remains large for most of the orbit, $\gtrsim$ 10 AU for ϕ between 0.5 and 0.925. However, between $\phi \approx 0.925$ and 1.0 (periastron), the separation drops rapidly, from $\sim$ 10 AU to 1.24 AU. At $\phi \sim 0.97$, the separation is $\sim$ 5 AU, which is about the same size as η_A in the K-band. Therefore, for the wavebands considered here, a bore-hole effect should occur in η Car at phases $0.97 \lesssim \phi \lesssim 1.03$.

Because of the different photospheric radii in each waveband, the wind cavity will bore different relative distances into η_A at a given ϕ in a particular waveband. Thus, at $\phi = 0.98$, one would expect to see a significant bore-hole effect in the K-band, but only a relatively minor effect, if any, in the B-band. Moreover, because of the differences in relative flux probed between wavebands, one might also expect different relative changes in brightness before, during, and after periastron.

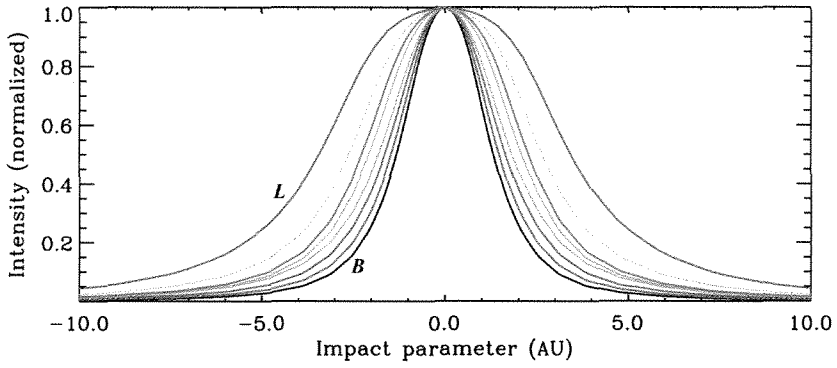

Figure 1. Curves showing normalized intensity vs. impact parameter in each of the wavebands (from innermost to outermost) *B, V, R, I, J, H, K, L*, computed using the H01, H06 `CMFGEN` model of η_A.

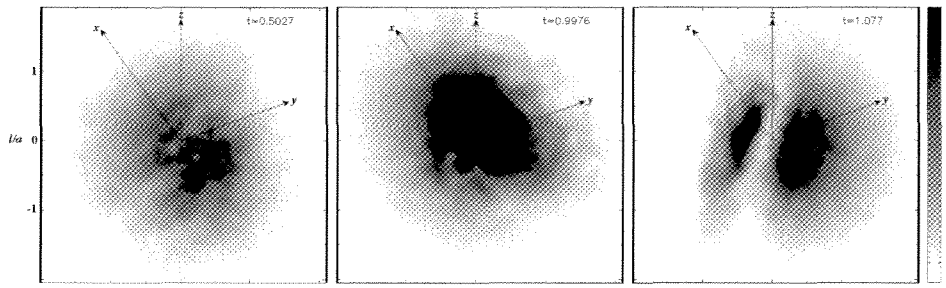

Figure 2. 3-D renderings of the bore-hole effect at orbital phases of apastron (left), 5 days before periastron (middle), and 155 days after periastron (right). The x and y axes are the major and minor axes, respectively, and z is the orbital axis $\perp$ to the orbital plane. Lengths are in semi-major axes and grayscale indicates surface brightness. See Madura (2010) for modeling details.

To investigate the bore-hole effect, we use 3-D SPH simulations of η Car's colliding winds, together with a modified version of the visualization program SPLASH (Price 2007), to generate renderings of the surface brightness of η_A in each of the various wavebands B through L as a function of orbital phase. Opacities and primary star source functions as a function of radius in each waveband were taken from the spherically symmetric model of η_A by H01, H06. Details can be found in Madura (2010).

Our models reveal that when η_B is at or near apastron, the WWIR is indeed too far from η_A and there is no bore hole (Fig. 2, left panel). As η_B moves closer to η_A during its orbit, the WWIR gradually penetrates into the primary photosphere, creating a bore-hole effect that increases up until periastron passage (Fig. 2, middle panel), at which point η_B quickly wraps around the back side of η_A, the bore hole briefly vanishing as it faces away from the observer. After periastron, the bore hole reappears on the opposite side of η_A (Fig. 2, right panel) and then slowly fades as η_B moves back toward apastron.

Using the above 3-D model, we also generate synthetic photometric light curves in each waveband for comparison to the available ground-based photometry (Whitelock et al.

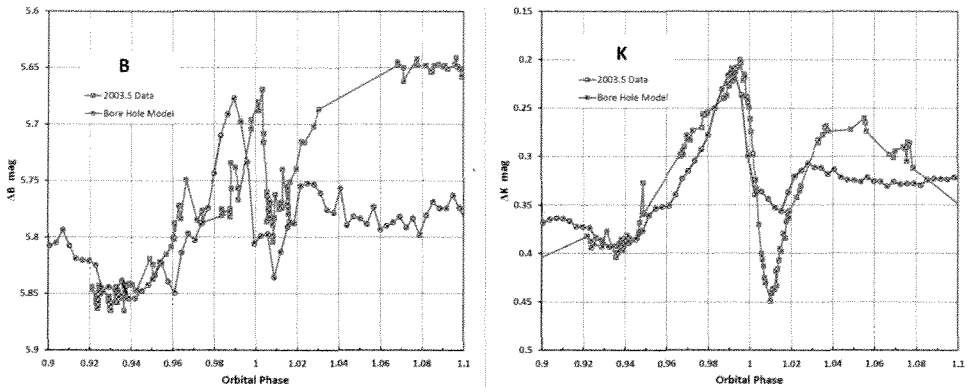

Figure 3. Synthetic light curves from the bore-hole model (circles) compared to the photometric observations of η Car's 2003.5 event (squares, Fernández-Lajús et al. 2010) in the B (left) and K (right) bands .

2004; Fernández-Lajús et al. 2010). We find that our bore-hole model reproduces the steep rise and drop observed in each waveband before periastron, and gives roughly the same peak-to-peak change in magnitude and duration of the 'eclipse-like' events seen every 5.54-years (see Figure 3 and Madura 2010). We thus find that η_B and the WWIR have a profound influence on η_A's extended photosphere and the photometric observables. The bore-hole effect likely explains η Car's periodic eclipse-like events.

3. Effects of a Bore Hole on η Car's Spectrum and Interferometric Observables

Using the 2-D code of Busche & Hillier (2005), we have also investigated how a bore-hole effect could alter the observed optical and UV spectra of η Car. Details on the modeling approach can be found in Groh (2011) and references therein.

Assuming a single-star scenario, H01 obtained a reasonable fit to the observed *HST* optical spectrum obtained just after periastron, $\phi \sim 0.05$. The model spectrum from H01 reproduces well the emission line profiles of H, Fe II, and N II lines. However, compared to the observations, the H01 model overestimates the amount of P-Cygni absorption. The comparison is even worse as one moves toward apastron, when the observations show little or no P-Cygni absorption in H and Fe II lines.

Using our 2-D radiative transfer model, which takes into account the cavity in the wind of η_A caused by η_B, we computed the synthetic optical spectrum of η Car at $\phi \sim 0.6$ (see figure 1 of Groh 2011). We assume the same parameters for η_A as H01 and a standard geometry of the WWIR at apastron as predicted by the 3-D SPH simulation. For a viewing angle with inclination $i = 41°$ and longitude of periastron $\omega = 270°$, the 2-D model produces a much better fit to the P-Cygni absorption line profiles of H and Fe II lines than the 1-D H01 model, while still fitting the emission line profiles. The improved fit to the P-Cygni absorption is due to the cavity in the wind of η_A, which reduces the H and Fe II optical depths in line-of-sight to the primary. We find similar results when modeling η Car's observed UV spectrum.

A preliminary study of synthetic Hα line profiles generated using our 2-D cavity model of η_A also reveals broader, deeper P-Cygni absorption near the stellar poles,

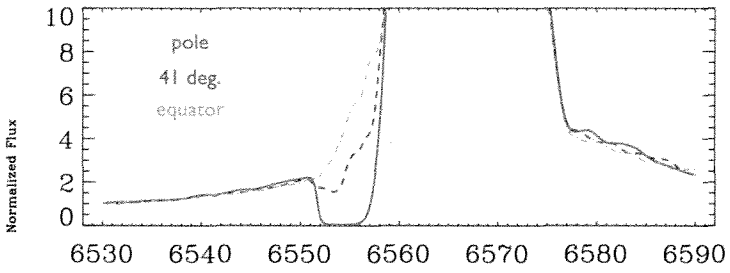

Figure 4. Synthetic line profiles of Hα generated using the 2-D model discussed in the text, emphasizing the P-Cygni absorption at three stellar latitudes for η_A.

compared to the equator (Figure 4). A bore-hole or wind-cavity model may therefore provide an alternative explanation for *HST* long-slit spectral observations of Hα line profiles as a function of stellar latitude that have been historically interpreted as evidence that the wind of η_A is latitude dependent (Smith et al. 2003).

Finally, using a similar 2-D model, Groh et al. (2010) find that the density structure of η_A's wind can be sufficiently disturbed by η_B and the associated wind cavity, thus mimicking the effects of fast rotation in the interferometric observables. Groh et al. (2010) further show that even if η_A is a rapid rotator, models of the interferometric data are not unique, and both prolate- and oblate-wind models can reproduce current interferometric observations. These prolate- and oblate-wind models additionally suggest that the rotation axis of η_A would not be aligned with the Homunculus polar axis.

4. Conclusions

Our conclusions are rather straightforward; based on the results of our 3-D hydrodynamical simulations and multi-D radiative transfer modelling, we find that the secondary star η_B and WWIR *significantly* affect the extended wind photosphere of η_A, and thus multi-wavelength observations of the η Car system.

Acknowledgments. We thank Nathan Smith for discussions that led to this work.

References

Busche, J. R. & Hillier, D. J. 2005, AJ, 129, 454
Corcoran, M. F. 2011, Bulletin de la Societe Royale des Sciences de Liege, 80, 578
Damineli, A. et al. 2008a, MNRAS, 384, 1649
Damineli, A. et al. 2008b, MNRAS, 386, 2330
Fernández-Lajús, E. et al. 2010, New Astronomy, 15, 108
Groh, J. 2011, Bulletin de la Societe Royale des Sciences de Liege, 80, 590
Groh, J. H., Madura, T. I., Owocki, S. P., Hillier, D. J., & Weigelt, G. 2010, ApJL, 716, L223
Hillier, D. J. et al. 2006, ApJ, 642, 1098 (H06)
Hillier, D. J., Davidson, K., Ishibashi, K., and Gull, T. 2001, ApJ, 553, 837 (H01)
Madura, T. I. 2010, Ph.D. Thesis, University of Delaware
Okazaki, A. T., Owocki, S. P., Russell, C. M. P., & Corcoran, M. F. 2008, MNRAS, 388, L39
Price, D. J. 2007, Publications of the Astronomical Society of Australia, 24, 159
Smith, N., Davidson, K., Gull, T. R., Ishibashi, K., & Hillier, D. J. 2003, ApJ, 586, 432
Whitelock, P. A., Feast, M. W., Marang, F., & Breedt, E. 2004, MNRAS, 352, 447